

FLOW-3D SOLIDIFICATION/MELTING UPDATE

C.W. Hirt and R.P. Harper
9/25/88

PURPOSE

The 1988 released version of FLOW-3D contained a simple model for representing solidification and melting phenomena. The essential feature of this model was a capability for driving the fluid velocity in a computational cell to zero when the cell temperature is below the solidification temperature. Implementation of this feature in the code was accomplished through a drag force proportional to velocity and having a temperature-dependent coefficient. A transition from no drag to infinite drag was introduced as the temperature T fell from the limit of all liquid, $T=TL1$, to the limit of all solid, $T=TS1$. It was a requirement of the model that the "liquidus" temperature, $TL1$, be greater than the "solidus" temperature, $TS1$.

A major deficiency of this model is that it does not account for latent heat associated with the phase transition. We have now implemented a code modification that accounts for latent heat and allows for different values of specific heat and thermal conductivity in the two phases. The new model also distinguishes porous media drag from "solidification drag" so that solidification/melting phenomena can be included as an additional effect in porous media flow.

In this note the new model is described and illustrated with several examples. Assumptions and limitations of the model are first explained in the next section, followed by a description of the new input parameters needed for its proper use. The last section contains sample calculational results that show how the new model may be coupled with a variety of other capabilities in FLOW-3D. One example is a comparison with experimental data and serves as a validation check on the new model.

ASSUMPTIONS AND LIMITATIONS

The solidification/melting model is based on several assumptions that must be clearly understood if it is to be used correctly. One assumption is that only fluid "one" (i.e., the fluid with volume fraction F) can undergo a phase transition. All FLOW-3D options, including the one-fluid free surface case, the incompressible two-fluid case, or the one compressible and one incompressible fluid case can be used in connection with the new model. In all cases, however, it is only the incompressible "F-fluid" that undergoes a phase transition.

A second basic assumption is that there is only one temperature associated with each computational mesh cell. Because the drag force used to keep solidified material at rest depends on temperature, this assumption also implies that in two-fluid problems no fluid of type 1 or 2 can flow in a cell if its temperature is below the solidus temperature and the cell contains some number 1 fluid. Requiring solidified material to be at rest additionally means that the model cannot handle situations involving moving chunks of solid.

A further assumption is that the specific heat of the solid phase must be equal to or greater than the specific heat of the liquid phase. This is physically realistic for any normal material will have more atomic and molecular degrees of freedom for storing energy in a solid state than in a liquid state. Finally, the latent heat of fusion cannot be zero when there is a nonzero transition temperature range, i.e., when TL_1 is greater than TS_1 . If this restriction were not imposed, it would be possible to have the entire range of temperatures from TS_1 to TL_1 associated with a single internal energy.

In the new model it is permissible to set TL_1 and TS_1 equal so that the phase transition occurs discontinuously at this temperature. When initializing a problem, however, if TL_1 is equal to TS_1 and the initial temperature is also equal to TS_1 , the code will assign an internal energy to the fluid as though it were all liquid at the melt temperature.

INPUT PARAMETERS FOR THE NEW MODEL

There are five new input parameters in Namelist XPUT needed to use the new solidification/melting model:

<u>Parameter</u>	<u>Default</u>	<u>Definition</u>
TS1	0.0	Solidus temperature (100% solid).
TL1	TS1	Liquidus temperature (100% liquid).
CVS1	CV1	Specific heat for solid phase of fluid number 1.
CLHT1	0.0	Latent heat of fusion for fluid number 1.
THCS1	THC1	Thermal conductivity for solid phase of fluid number 1.

To activate the model it is only necessary to set TS1 to a nonzero value. Note that this is different from the 1988 code where IDR_G was set equal to 3 to initiate the solidification process. Actually, IDR_G=3 will still work provided the remaining parameters have been properly set, but in this case ADR_G and BDR_G no longer control the temperature-dependent drag because porous media and solidification processes are now distinguished from one another.

In any case, the minimum input necessary to use the new model is a nonzero value of TS1. If none of the remaining parameters defined above are set in the input file, then a phase transition will occur at temperature $T=TS1$ with zero latent heat and with the solid specific heat and thermal conductivity values equal to their liquid-phase values.

ILLUSTRATIVE EXAMPLES

We illustrate this new capability with a simple natural convection problem defined in nondimensional units. A cubical cavity with edge length 1.0 is constructed with insulated walls on its front, back, top and bottom sides. The left wall is given a constant temperature of 1.0, while the right wall is assigned a constant temperature of 0.0. The heat transfer coefficient for both of these walls is 20. Gravity acts downwards (parallel) to

the heated and cooled walls with magnitude $-7.1E+4$. Fluid in the cavity has a nominal density of 1.0, a thermal expansion coefficient of 0.01, a molecular viscosity of 0.71 and a thermal conductivity of 1.0. These parameters correspond to a Rayleigh number for natural convection of 1000.

No Phase Change

In the absence of phase change, liquid in the cavity will develop a clockwise, two-dimensional, natural circulation between the specified temperature walls that eventually reaches a steady state. Figure 1 shows the flow velocity field and temperature contours at $t=0.1$, which is nearly, but not quite, at steady state conditions. A relatively small 10 by 10 cell mesh was used for this demonstration problem.

Solidification Test

To investigate the effects of adding a phase change we next set the solidus and liquidus temperatures equal to 0.33 (i.e., $TS1=TL1=0.33$), the latent heat to $CLHT1=0.2$, and the solid phase parameters $CVS1=1.2$ and $THCS1=1.2$. With an initial temperature in the cavity of 0.5 the computed results at $t=0.1$ are those shown in Fig. 2. Here it is evident that the fluid has solidified in the three mesh cells at the right side of the cavity. Referring to the temperature contours it is verified that this is the region where T is less than the solidus temperature.

Figure 3 contains the temperature histories computed at the lower left and lower right corners of the cavity. The lower left corner shows a monotonic temperature increase. The lower right corner, on the other hand, exhibits a monotonic decrease with a temperature plateau at the solidification temperature $T=0.33$. This plateau indicates the presence of latent heat that must be removed before the material can further cool. The change in cooling rate around $t=0.02$ results from a change in the relative influence of natural convection and conduction processes.

Melting Test

A repeat of the last problem, but with an initial temperature of $T=0.25$, which is below solidus temperature, shows that melting can be modeled as well as solidification. In this

case, Fig. 4, the melting front has propagated further across the cavity from the hot wall than the freezing front propagated from the cold wall in the previous example. Given enough time both calculations will, of course, converge to the same steady state. The differences observed at $t=0.1$ are a consequence of using an initial temperature closer to the fusion temperature in the melting case than in the freezing case (0.08 degrees versus 0.12 degrees).

Two-Fluid Test

To show how the new model might be used in a two-fluid situation, a horizontal interface was defined midway in the cavity with the top fluid (fluid number 2) having a lower density of 0.9, but otherwise the same physical properties as the lower fluid. Starting with an initial temperature of $T=0.5$ the calculated flow at $t=0.1$ is shown in Fig. 5. Here it is only fluid 1 below the interface that solidifies near the cold boundary. Separate convection cells are generated above and below the interface because the interface density is too large to be significantly displaced by the relatively weak thermal buoyancy.

Experimental Data Comparison

A more demanding test of the new solidification/melting model is to make comparisons with experimental data. Locating suitable data, however, is often difficult particularly when phase changes are involved. Fortunately, there exist published data for an ideal test problem. The data, obtained by Gau and Viskanta [1], concerns the propagation of a melting front through a frozen mass of gallium.

The experimental arrangement is quite similar to the two-dimensional cavity problems already considered. A rectangular region 8.89 cm wide and 6.35 cm high is filled with gallium at 28.3° C. The top, bottom, front and back sides of the region are insulated. The right side is held at the initial temperature, while the left side is held at a temperature of 38° C. Since the melting temperature of gallium is 29.78° C, the metal begins to melt along the left wall, and with time natural convection sets in enhancing the transport of heat to the melt front. Natural convection, which is important in this problem, causes the melt front to develop a strong two-dimensional shape. Since the front can be experimentally measured, and because its location and shape depend on both conduction and convection, it is a good

feature to use for comparison with computations.

The data of Gau and Viskanta has previously been used for comparison with a computational model used by Brent, et al [2]. For the present test we have used the same physical parameters used by these authors, which in CGS units are:

Density	6.095
Melt temperature	29.78° C
Latent heat	8.02E+8
Thermal expansion coefficient	1.2E-4
Specific heat	3.815E+6
Thermal conductivity	3.2E+6

The reference temperature for buoyancy is the same as the melt temperature. No mushy zone is needed for pure gallium so the liquidus and solidus temperatures are also equal to the melt temperature. Conduction at the left and right walls is assumed to be perfect, which makes the wall heat transfer coefficients equal to the liquid thermal conductivity divided by one half the mesh cell size in the horizontal direction (in others words, pure conduction with wall temperatures specified at the cell edge).

The mesh consisted of 30 cells in the horizontal (X) direction, 20 cells in the vertical (Z) direction and 1 cell in the Y direction (for a two-dimensional representation). The mesh cells were all of equal size. This is somewhat smaller than the mesh used in Ref. 2, but inspection of the data suggested that this would be sufficient.

Velocity and temperature contours at selected times are displayed in Fig. 6. The location of the solid/liquid boundary is clearly evident in the velocity plots. As time proceeds the increased heat transfer at the top of the cavity by natural convection is obvious. It should also be noted in this connection that the largest temperature gradients are located at the top of the melt front and at the foot of the heated wall where cold fluid is returning to be reheated.

To define the melt front location we followed a procedure analogous to that used by Brent, et al, which was to identify the front with the location of internal energy midway between all liquid and all solid states. In fact, referring to Fig. 7, which shows the contours of internal energy per unit volume midway into the calculation, we see that there is little variation in energy except at the melt front. Therefore, almost any energy value in

the melt zone would provide a good estimate of the liquid/solid interface location. This close packing of energy contours is a consequence of the large latent heat of gallium.

A comparison of the computed melt front location with the experimental data and with the computational results given in Ref. 2 is shown in Fig. 8 (this is figure 9 from Ref. 2 with the FLOW-3D results plotted as dots). We see that FLOW-3D gives results in excellent agreement with the experimental data. In most places the offset between FLOW-3D predictions and data is less than the width of one computational cell (see lower right corner for the mesh cell size).

For this computation we elected to use the purely explicit heat transfer calculation option in FLOW-3D. Our motivation for doing this was to be sure of an accurate solution even if a longer computational time was required. In retrospect, however, we discovered that the maximum stable time-step limit for fluid advection is very close to the time-step limit for heat conduction so that the implicit heat transfer option would not have reduced the computational time. This finding emphasizes the importance of natural convection in this example. The total computational time on a MicroVAX II computer to reach a problem time of 20 minutes was 57.48 hours.

Since this CPU time seems somewhat larger than that reported in Ref. 2 (direct comparisons cannot be made because different computers were used), it may be useful to consider the reasons why this is the case. In Ref. 2 a fully implicit computational procedure was used to solve all the governing equations. The implicit solution procedure requires iterations within each time step that are roughly comparable with our explicit time steps. Based on the reported average number of iterations (43) and time-step size of 10 sec, the effective explicit time-step size used in Ref. 2 was 0.23 sec. This value is about three times the stable limit for explicit conduction and about 4.6 times the limit for explicit convection. In general, in time-dependent problems implicit methods tend to lose accuracy as the explicit stability limits are exceeded. This loss of accuracy does not seem particularly apparent in the results of Brent, et al, and we believe this is because of the large latent heat. Having to remove the latent heat takes time, which slows down the transient evolution of the melt front. In effect, the presence of a large latent heat allows the flow to adjust to quasi-steady conditions during the melting of each new set of computational zones. Such CPU savings, unfortunately, may not be possible in other problems involving smaller latent heats, larger temperature differences or free surfaces, which must be evolved in a more explicit way.

Another reason for an increased computational time in FLOW-3D may be our use of a three-dimensional code for this two-dimensional problem, which adds some computational overhead. In any case, considering the difficulty of physical problem and the accuracy of the results the computational effort is quite reasonable.

REFERENCES

1. Gau, C. and Viskanta, R., "Melting and Solidification of a Pure Metal on a Vertical Wall," J. Heat Transfer 108, 174 (1986).
2. Brent, A.D., Voller, V.R., and Reid, K.J., "Enthalpy-Porosity Technique for Modeling Convection-Diffusion Phase Change: Application to the Melting of a Pure Metal," Num. Heat Transfer 13, 297 (1988).

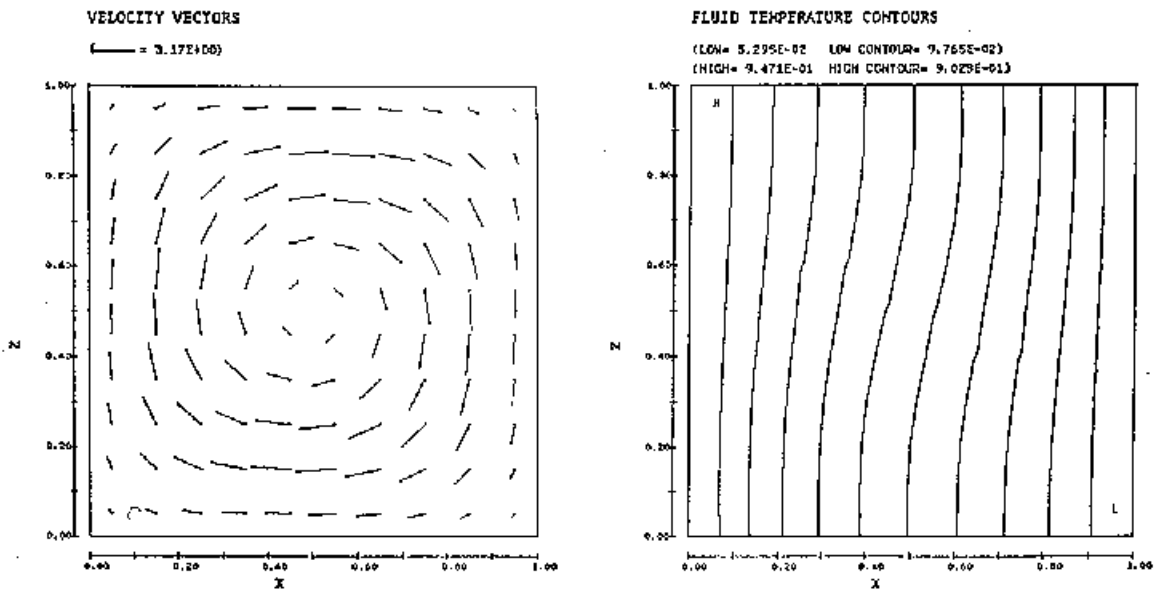


Fig. 1. Natural Convection without phase change at $t=0.1$.

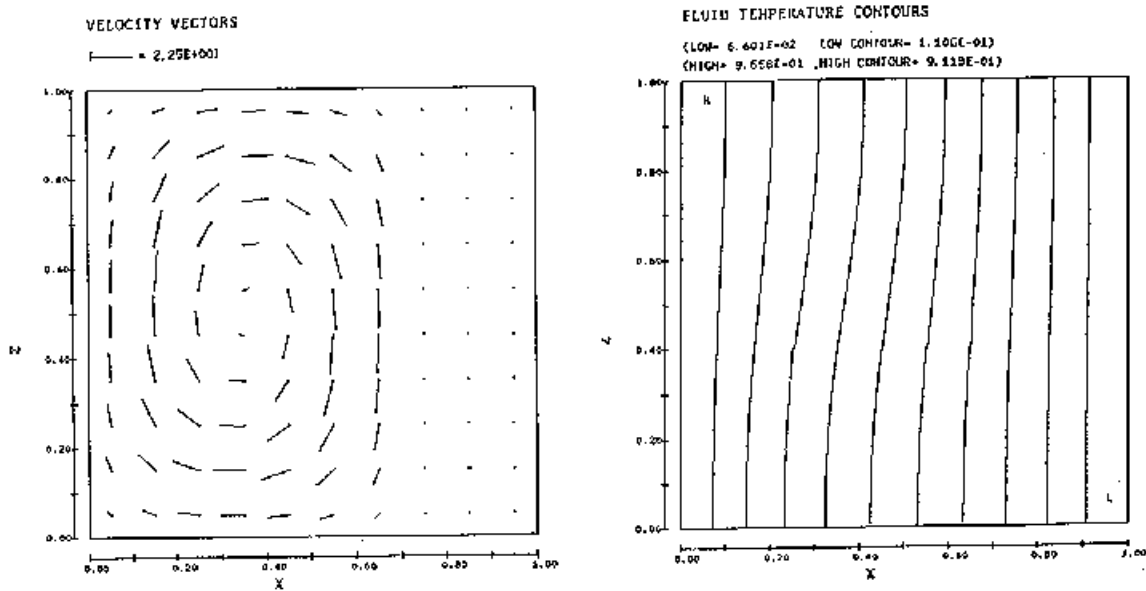


Fig. 2. Solidification from right boundary at $t=0.1$.

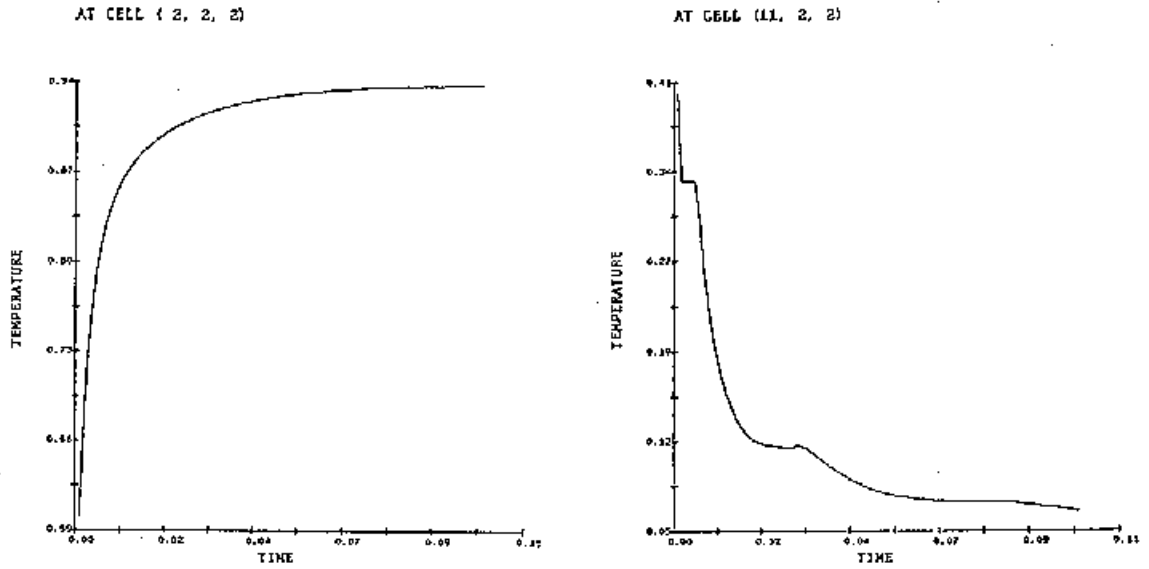


Fig. 3. Temperature histories for solidification test at lower left corner (left) and lower right corner (right).

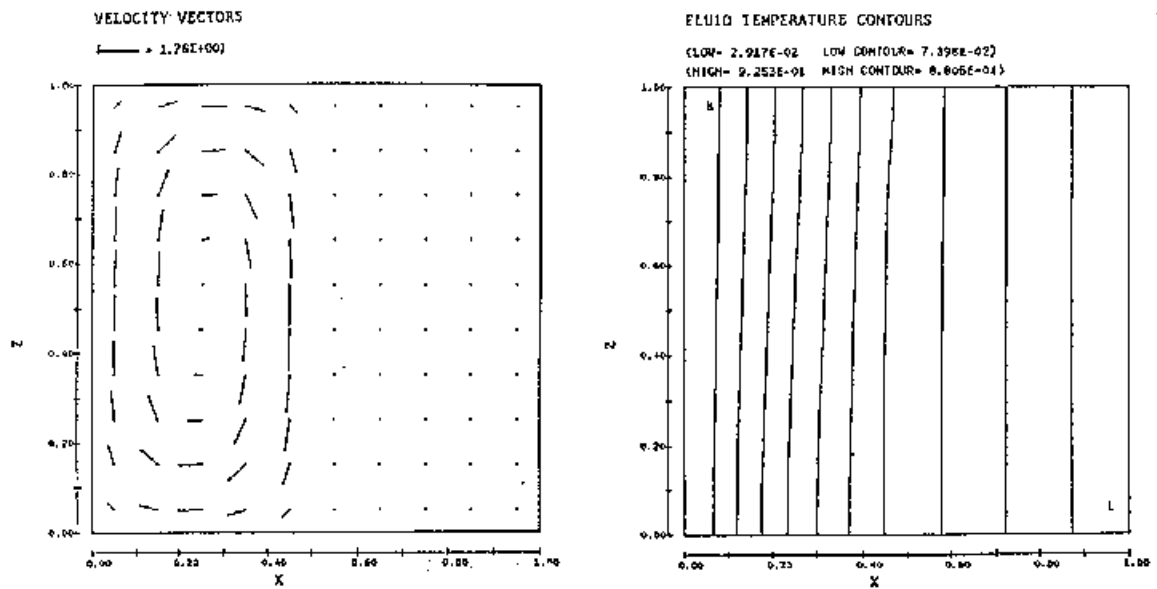


Fig. 4. Melting from left boundary at $t=0.1$.

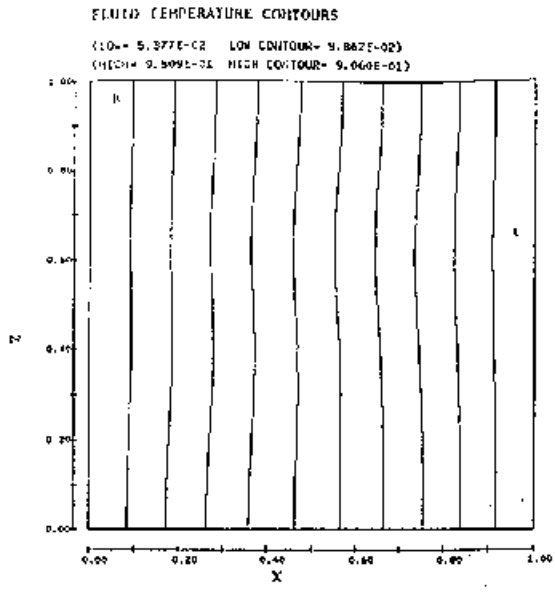
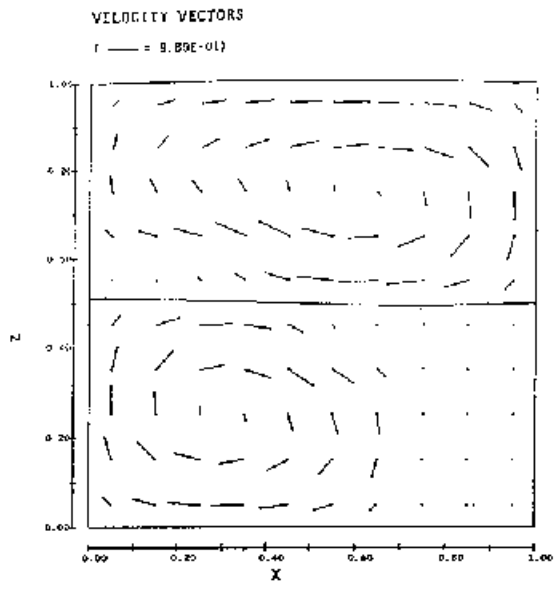


Fig. 5. Two-fluid test with solidification occurring at right boundary in lower fluid. Time is 0.1.

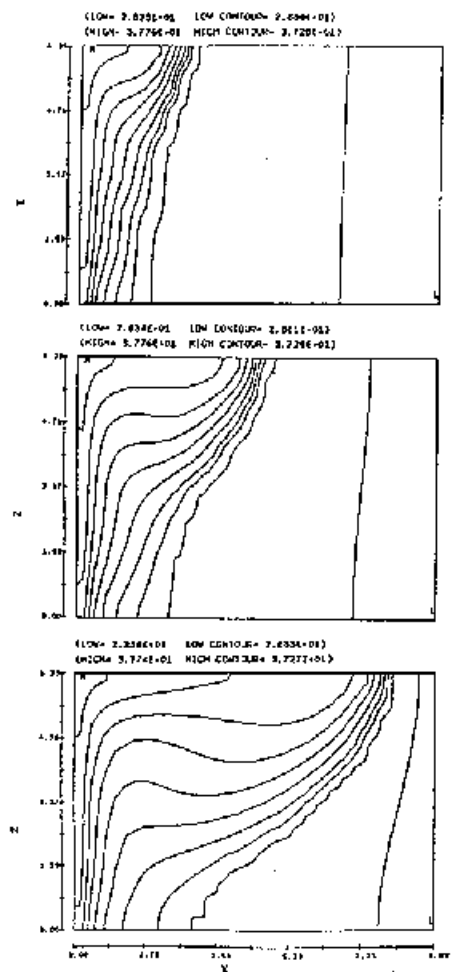
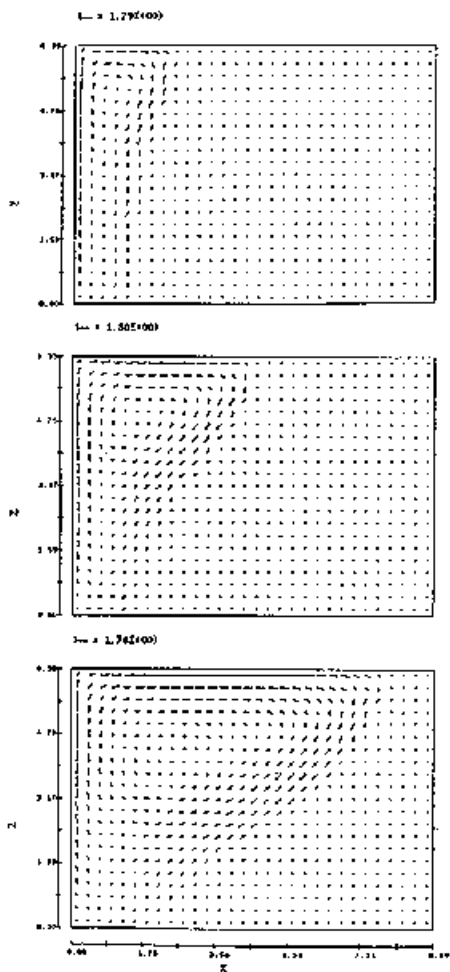


Fig. 6. Velocity fields and temperature contours computed for comparison with Ref. 1. Times, from top to bottom, are 300, 600 and 1200 seconds.

ENERGY CONTOURS

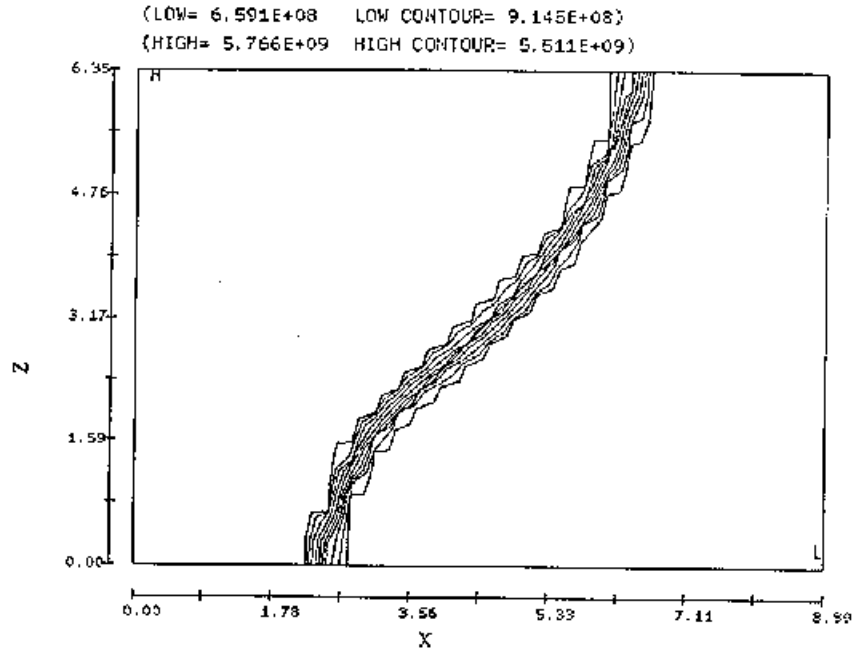


Fig. 7. Energy Contours computed at 15 min.

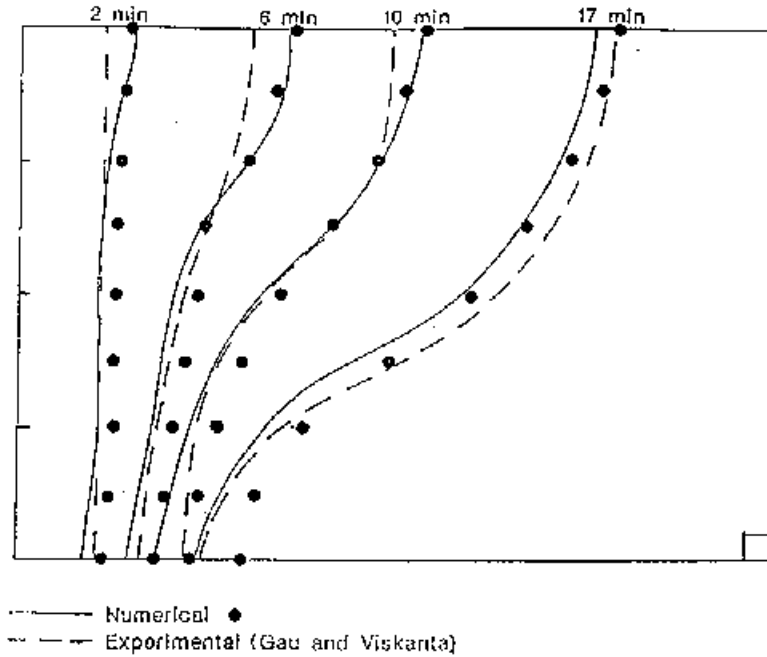


Fig. 8. Comparison of computed melt front with experimental data. (From Fig. 9 of Ref. 2.) Dots indicate FLOW-3D results.